Current Biology, Vol. 15, 1266–1275, July 26, 2005, ©2005 Elsevier Ltd All rights reserved. DOI 10.1016/j.cub.2005.06.062

Regulation of Lipid-Droplet Transport by the Perilipin Homolog LSD2

Michael A. Welte,[1,2,6] Silvia Cermelli,[5,6] John Griner,[1] Arturo Viera,[5] Yi Guo,[1,3] Dae-Hwan Kim,[1,2] Joseph G. Gindhart,[4] and Steven P. Gross[5,*]
[1]Rosenstiel Biomedical Research Center
[2]Department of Biology
[3]Department of Biochemistry
Brandeis University
415 South Street
Waltham, Massachusetts 02454
[4]Department of Biology
University of Richmond
28 Westhampton Way
Richmond, Virginia 23173
[5]Department of Developmental and Cell Biology
2222 Natural Sciences I
University of California, Irvine
Irvine, California 92697

Summary

Background: Motor-driven transport along microtubules is a primary mechanism for moving and positioning organelles. How such transport is regulated remains poorly understood. For lipid droplets in *Drosophila* embryos, three distinct phases of transport can be distinguished. To identify factors regulating this transport, we biochemically purified droplets from individual phases and used 2D gel analysis to search for proteins whose amount on droplets changes as motion changes.
Results: By mass spectrometry, we identified one such protein as LSD2. Similar to its mammalian counterpart Perilipin, LSD2 is responsible for regulating lipid homeostasis. Using specific antibodies, we confirmed that LSD2 is present on embryonic lipid droplets. We find that lack of LSD2 causes a specific transport defect: Droplet distribution fails to undergo the dramatic changes characteristic of the wild-type. This defect is not due to a complete failure of the core transport machinery—individual droplets still move bidirectionally along microtubules with approximately normal velocities and kinetics. Rather, detailed biophysical analysis suggests that developmental control of droplet motion is lost. We show that LSD2 is multiply phosphorylated in a developmentally controlled manner. LSD2 phosphorylation depends on the transacting signal Halo, and LSD2 can physically interact with the lipid-droplet-associated coordinator Klar, identifying LSD2 as a central player in the mechanisms that control droplet motion.
Conclusions: LSD2 appears to represent a new class of regulators, a protein that transduces regulatory signals to a separable core motor machinery. In addition, the demonstration that LSD2 regulates both transport and lipid metabolism suggests a link between lipid-droplet motion and lipid homeostasis.

*Correspondence: sgross@uci.edu
[6]These authors contributed equally to this work.

Introduction

Motor-driven transport along microtubules positions and delivers many cellular organelles, including the ER, Golgi, mitochondria, axonal vesicles, and nuclei. Many cargoes move in a bidirectional manner: They engage in repeated short back-and-forth movements [1, 2], alternately using plus-end (e.g., kinesin-1 and kinesin-2) and minus-end motors (typically cytoplasmic dynein). Net, or average, transport depends on the balance of plus- and minus-end-directed motion.

Such transport is often dynamically regulated. For example, mitochondria move to growth cones where ATP is needed [3]; viruses change their motion between initial infection and subsequent spread [4, 5]; and pigment granules disperse or aggregate to camouflage fish or frogs [6]. The motion of different cargoes in the same cell can be controlled independently, although the cargoes move in the same cytoplasm and often employ the same set of motors. Thus, multiple levels of regulation control timing, direction, and cargo specificity of transport.

In a few model systems, key transport regulators have been identified. For example, net pigment granule transport is controlled by protein kinase A [7, 8], and mitochondrial accumulation requires signaling through the PI-3 kinase pathway [3, 9]. However, the downstream targets of these kinases are not known.

To dissect these regulatory mechanisms, we investigated lipid-droplet motion in early *Drosophila* embryos. Past work with genetic, molecular, and biophysical approaches identified four molecules important for droplet transport: the minus-end motor cytoplasmic dynein [10] and its cofactor dynactin [11], the proposed coordinator Klar [12, 13], and the transacting signal Halo [14]. How these molecules work together mechanistically has not yet been established. Halo is a novel molecule of unknown molecular function. Klar is physically associated with lipid droplets, and lack of Klar appears to cause a breakdown in motor coordination, yet Klar's sequence has provided few mechanistic insights. Finally, unlike in other systems, there is as yet no evidence that protein kinases play roles in regulating droplet motion.

Lipid droplets are not a specialization of *Drosophila* embryos. They are ubiquitous organelles present in most eukaryotic cells, from yeast to plants to mammals [15–17]. As the predominant cellular storage site for neutral lipids, lipid droplets play central roles for energy metabolism, steroid biogenesis, and diet-induced obesity. Yet despite their biological importance, protein components of droplets have been identified only fairly recently, and the cell-biological study of lipid droplets is in its infancy. For example, lipid droplets actively move along microtubules in cells from *Drosophila* to fish to mammals [12, 18–20], but the functional significance of this motion is unclear.

Here, we use a biochemical/proteomic approach to identify potential regulators of droplet transport in *Drosophila* embryos. We show that LSD2, lipid storage

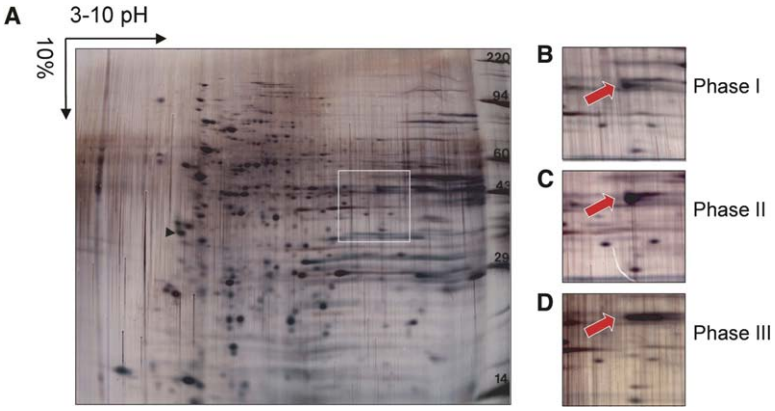

Figure 1. Protein Profile of Isolated Lipid Droplets

Fifty micrograms of total protein from purified lipid droplets was subjected to 2D gel electrophoresis and then silver stained.

(A) Whole gel of phase 0 lipid droplets. The black arrowhead corresponds to the isoelectric focusing (IEF) internal standard, tropomyosin. The molecular weight standards are indicated to the right. One of the spots at 44 kDa and pI 8.1 was observed to undergo intensity changes according to the developmental phase. This region of the gel is indicated in (A) and shown in detail in panels (B)–(D). This spot (red arrow) was low in phase I (B), increased in phase II (C), and was lower again in phase III (D). This spot was excised and, by mass-spectroscopy, identified as LSD2.

droplet protein 2, is present on embryonic lipid droplets and that lack of LSD2 results in a specific transport defect: A core transport machinery is intact because motors remain attached to the droplets and function relatively normally, but regulation of motion is prevented. We find that LSD2 is multiply phosphorylated in a developmentally controlled manner, that changes in its phosphorylation state depend on the Halo protein, and that Klar and LSD2 can physically interact. These observations suggest that LSD2 is a crucial link between developmental signals (like Halo) and the core motor machinery, whose activity it modifies. Because LSD2 also plays a central role in lipid metabolism [21, 22], our results suggest a possible link between droplet motion and the regulation of metabolism. This connection might be quite general because droplets in many organisms move, and the mammalian homolog of LSD2—Perilipin—also controls lipid homeostasis.

Results

Physical Isolation and Separation of Lipid-Droplet Proteins

Lipid droplets are composed of a layer of phospholipids and proteins surrounding a central core of neutral lipids [15]. To characterize proteins physically associated with the droplets, we first purified the droplets from *Drosophila* embryos with a protocol almost identical to the flotation method from Yu et al. [23]. Details of this procedure will be published elsewhere (S. Cermelli et al., unpublished data).

After resuspension, proteins were separated by molecular weight and/or isoelectric point and then detected by in-gel staining or Western blotting. Silver staining of typical droplet preparations revealed several hundred spots (Figure 1). We believe that many of them represent bona fide droplet-associated proteins because by Western analysis, markers for several other organelles were either absent or highly depleted in these samples (S. Cermelli et al., unpublished data).

A Droplet-Associated Protein Whose Levels Change during Development

Throughout the first few hours of *Drosophila* embryogenesis, lipid droplets move bidirectionally along microtubules, and net transport changes reproducibly [12]. Phase I, with no net transport, is followed by net plus-end transport (phase II) and subsequently by net minus-end transport (phase III).

One potential mechanism to regulate motion is a change in the protein composition of the droplets. We therefore isolated lipid droplets from staged collections of wild-type embryos (see Experimental Procedures). Droplet proteins were separated on 2D gels and visualized with silver staining (Figure 1A). The overall spot pattern was similar for all phases, but there was a consistent change: One spot was faint in phase I, strong in phase II, and of intermediate intensity in phase III (Figures 1B–1D, arrow). This pattern repeated in three independent experiments. The relevant spot was excised, and its identity was determined by mass spectrometry to be lipid storage droplet protein 2, LSD2. LSD2 is a member of the PAT protein family of lipid-droplet-associated proteins present in species from mammals to slime molds [24]. One of the mammalian family members, Perilipin, functions as a gateway molecule in neutral-lipid metabolism in adipocytes [25]. Depending on its phosphorylation state, Perilipin prevents or promotes the docking of lipases to droplets and thus controls the breakdown of stored lipids. Insects generally have two family members [26], LSD1 and LSD2. In *Drosophila*, knockouts of LSD2 impair, but do not abolish, the ability of the animal to store neutral lipids [21, 22].

LSD2 Is Associated with Embryonic Lipid Droplets

To study LSD2's possible role in droplet transport, we employed several *LSD2* alleles. We focused on an RNA null allele, called $LSD2^{KG}$ here, that is due to a P element insertion [22]. In some experiments, we also used alleles Δ1 and Δ2, derived from $LSD2^{KG}$ and the independent P element allele $LSD2^{BG}$ (Figure 2A).

With an antibody against a C-terminal LSD2 peptide, we detected a protein of ~43 kDa in embryo lysates by Western analysis (Figure 2B), consistent with the size of LSD2 in larval tissues [22]. Genetic controls demonstrated that this band represents LSD2 (Figure 2B). LSD2 protein is maternally provided (see Figure S1 in the Supplemental Data available with this article online), and in comparison to embryo lysates, it is highly enriched in the droplet fraction (Figure 2C). In adult and

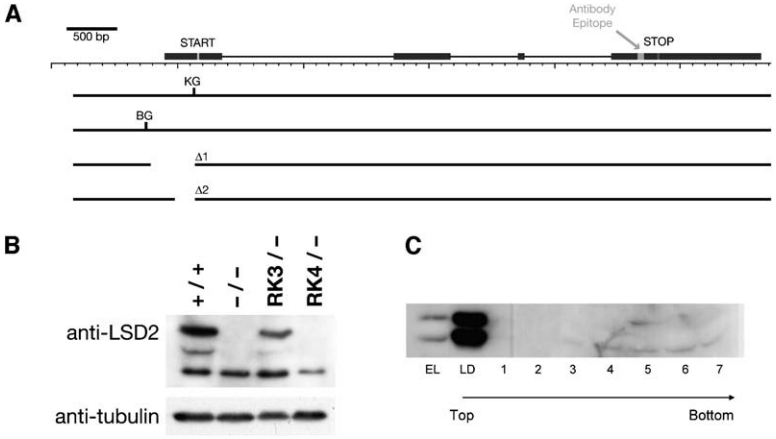

Figure 2. LSD2 Molecular Genetics and Protein Expression

(A) Structure of the *LSD2* gene. Top: genomic sequence and the exon/intron structure. Bottom: the four mutant chromosomes analyzed for this study. KG is a P element insertion (KG00149) in the 5′UTR; it is both an RNA null [22] and a protein null (see Figure 2B) allele. BG is the insertion BG00016 [21]; it shows variable defects in clearing and variable protein levels, and it appears to be a weak allele. Δ1 and Δ2 are two chromosomes derived from KG by P element excision; homozygotes express little to no protein and have clearing defects like KG (not shown).

(B) Expression of LSD2 by Western analysis. Proteins were extracted from phase II embryos laid by mothers of various genotypes: +/+ = wild-type; –/– = $LSD2^{KG}$ homozygotes; RK3/– = flies heterozygous for $LSD2^{KG}$ and *Df(1)RK3*, a chromosomal deletion that does not remove the *LSD2* gene. RK4/– = flies heterozygous for $LSD2^{KG}$ and *Df(1)RK4*, a chromosomal deletion that deletes the *LSD2* gene. Proteins were separated by SDS PAGE, transferred to membranes, and detected with antibodies against LSD2 (top) or tubulin (bottom). The anti-LSD2 antibody detects a major band in the wild-type; this band is absent in the genotypes lacking a functional *LSD2* gene.

(C) LSD2 is biochemically enriched on lipid droplets. Lipid droplets were purified by flotation with a sucrose gradient, and fractions were taken from the very top of the gradient (LD) where lipid droplets reside and from successively lower regions (1–7). Equal volumes of these fractions were loaded per lane, and LSD2 was detected as in (B). LSD2 was only detected in the top-most fraction, confirming that it is entirely localized to lipid droplets. A sample of total embryo lysates (EL, left) that contained the same amount of total protein (20 μg) as the LD fraction was loaded. LSD2 was highly enriched in the LD fraction in relation to the embryo lysate.

larval tissues, LSD2-GFP fusions localize to the surface of lipid droplets [22, 24], and endogenous LSD2 has been detected on lipid droplets in ovaries [21]. By immunostaining, we detected LSD2 throughout the periphery of embryos (Figure S2) in abundant round structures (Figure 3E) reminiscent in shape and size of lipid droplets. By four independent criteria, these structures are indeed lipid droplets: First, LSD2 signal was found throughout the periphery in phase I and accumulated basally in phase II (Figures 3B and 3C), just like lipid droplets [12]. Second, in embryos lacking the regulator Halo, both LSD2-positive structures (Figure 3D) and lipid droplets [14] accumulate apically instead of basally; other organelles are normally distributed [14]. Third, when embryos are centrifuged, lipid droplets and associated regulators such as Klar accumulate on one side of the embryo in a droplet layer [13]. LSD2 was also highly enriched in this layer (Figures 3F and 3G). Finally, when embryos were broken to disperse embryonic organelles, LSD2 signal (green) surrounded the droplets' neutral lipid core (red) (Figures 3H and 3I). Together with the Western data (Figure 2C), these observations argue that in embryos, LSD2 is largely present on lipid droplets. It is possible that a small fraction of embryonic LSD2 is present elsewhere; in larvae, LSD2 has been reported to partially localize to the ER [27].

Lack of LSD2 Results in Abnormal Droplet Distribution

To determine whether the absence of LSD2 affected lipid-droplet motion, we observed embryos from $LSD2^{KG}$ and wild-type mothers by video microscopy. Changes in droplet distribution cause changes in embryo transparency [12]: In the wild-type, net inward plus-end droplet motion (phase II) results in a transparent embryo periphery (clearing), and net outward minus-end motion (phase III) turns embryos opaque again (clouding). In $LSD2^{KG}$ embryos, the peripheral cytoplasm failed to clear completely in phase II; a brownish ring persisted around the central yolk throughout phase II (Figures 4A and 4B). This failure to clear was reminiscent of phase II $halo^{-}$ embryos in which apical droplet accumulation results in a broad brownish ring visible throughout the embryo periphery (Figure 4C). $LSD2^{KG}$ embryos were intermediate between $halo^{-}$ and wild-type (Figures 4A–4C). In reciprocal crosses between wild-type and $LSD2^{KG}$ flies, the failure to clear completely depended only on the genotype of the mother (data not shown), consistent with maternal loading of LSD2 protein into embryos. The failure to clear correctly is likely due to the lack of LSD2 because similar clearing defects are observed with the alleles $LSD2^{\Delta 1}$ and $LSD2^{\Delta 2}$ and more weakly and variably for the independently isolated allele $LSD2^{BG}$ (Figure 2A), which produces variable amounts of protein.

We stained embryos with the droplet-specific dye Nile red to directly compare the droplet distribution in wild-type and $LSD2^{KG}$. In phase II, droplets in wild-type embryos were localized basally, but they were distributed throughout the periphery of $LSD2^{KG}$ embryos (Figures 4D and 4E). In phase III, droplets were found throughout the embryo periphery in both genotypes (not shown). Thus, there is little, if any, net transport of droplets in *LSD2* mutant embryos.

Lack of LSD2 affects lipid homeostasis [21, 22] and, thus, might affect transport by generally impairing embryogenesis. However, embryonic development appeared normal in the mutant; $LSD2^{KG}$ embryos underwent cleavage, cellularization, gastrulation, and germband extension like the wild-type. Many embryos hatched, giving rise to fertile adults. The distribution of other cellular structures (nuclei, yolk, Golgi) was indistinguishable between wild-type and mutant embryos, suggesting that other motor-driven transport is unaffected (Figures 4F and 4H).

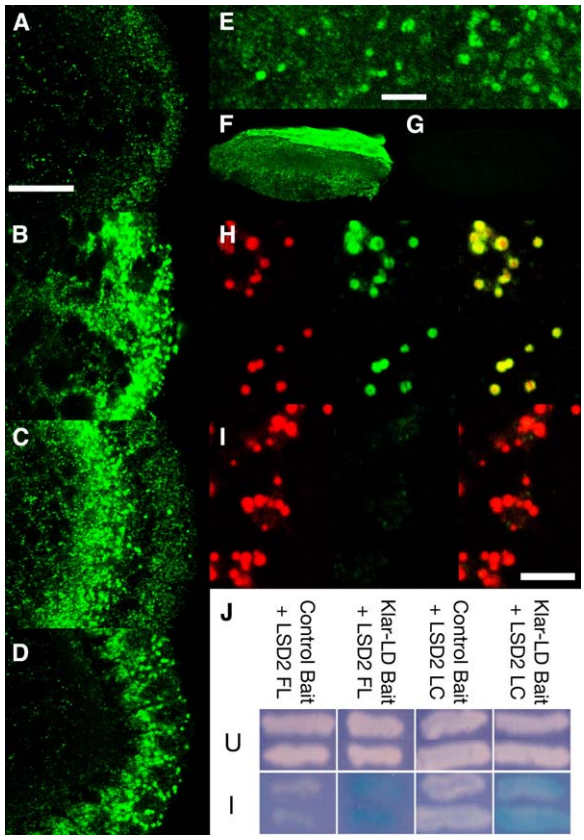

Figure 3. LSD2 Localizes to Lipid Droplets

(A–D) A closeup view of the embryo periphery (basal, left; apical, right) shows that LSD2 signal distribution is reminiscent of lipid droplets. (A) *LSD2*^{KG} phase II embryos show only background signal. (B) Wild-type phase I is shown; staining all over the periphery. (C) Wild-type phase II is shown; signal accumulates basally. (D) *Halo*$^{-}$ phase II embryos are shown; signal accumulates apically.

(E) Wild-type embryo, high-magnification view. LSD2 labels round structures the size of lipid droplets.

(F and G) Wild-type embryos centrifuged to enrich lipid droplets on the side of the embryo. Left, anti-LSD2, and right, primary antibody omitted. LSD2 is highly enriched in the lipid-droplet layer (top right in [F]), as detected by transmitted light microscopy (not shown).

(H and I) Lipid droplets were diluted away from other organelles by squashing wild-type (H) or *LSD2*^{KG} (I) embryos into buffer, fixed, and treated with the droplet-specific dye Nile red (red, left) and anti-LSD2 (green, middle). The right panels show the overlay between the two signals.

(J) LSD2 binds to the lipid-droplet targeting domain of Klar. Representative yeast colonies grown on X-gal plates are shown. Colonies were grown with glucose (U) or galactose (I) as a carbon source; glucose represses LSD2 prey transcription, whereas galactose induces it. Reporter-gene activity, as assayed by blue colony coloration, is enhanced in cells containing Klar-LD bait and either full-length LSD2 (LSD2 FL) or LSD2 aa 78–352 (LSD2 LC) on galactose media. Reporter-gene transcription is dependent upon Klar-LD because colonies containing a control bait and LSD2 are white. The scale bars represent 16 μm in (A) and 4 μm in (E) and (I).

Loss of LSD2 Affects Specific Parameters of Droplet Motion

If LSD2 were responsible for motor docking, its loss could lead to motorless droplets and, thus, lack of net droplet transport. However, in *LSD2*^{KG} embryos, droplets displayed vigorous bidirectional motion as in the wild-type (Figure 5), demonstrating that motors must still be present. Indeed, anti-dynein Western blots found similar amounts of dynein in droplet preparations from wild-type and *LSD2*^{KG} embryos (Figure 4G), and the pattern of dynein immunolocalization to droplets was similar between the two (Figure 4I). Thus, the motors are on the droplets but are incorrectly regulated in the absence of LSD2.

To clarify LSD2's function, we quantified droplet motion in *LSD2*^{KG} embryos and in a simultaneously acquired set of wild-type data. Droplets display periods of uninterrupted motion ("runs") interspersed with reversals in directions and pauses. In the wild-type, two classes of runs can be distinguished: short-slow runs (low velocities, short travel distances) and long-fast runs (higher velocities, longer travel distances). It is predominantly the long-fast runs that are regulated to control net transport. *LSD2* mutant embryos displayed both classes of runs, on the basis of previously established criteria [10, 11] (see Table 1). In phase II, both plus-end and minus-end run lengths were slightly decreased in relation to the wild-type (Figures 5A and 5B), but the decrease in plus-end motion was larger, resulting in abolishment of net transport. This decrease in average run length was due to a decrease in the length of long-fast runs, rather than a change in the relative number of long-fast versus short-slow runs (Table 1). To specifically measure the velocities of long-fast runs, we examined the mean velocity of runs between 500 and 1000 nm long because there are almost no short-slow runs longer than 300 nm [11]. For both directions, motion was slightly slower in mutant than in wild-type embryos (Figures 5C and 5D).

Strikingly, the developmental transitions characteristic of wild-type droplet motion failed to occur in the mutant. In the wild-type, the mean run length of plus-end motion decreases between phases II and III (Figures 5A and 5B), and the mean velocity of long plus-end and minus-end runs decreases slightly as well (Figures 5C and 5D). Neither of these changes occurred in *LSD2*^{KG} embryos, in which the parameters of motion in phases II and III were essentially the same (Figure 5; Table 1). Thus, loss of LSD2 function results in the inability to regulate droplet transport.

We conclude that without LSD2, the general machinery that powers droplet motion is intact because droplets move bidirectionally with approximately normal velocities, runs have roughly the correct lengths, and the ratio of short-slow to long-fast runs is close to that of the wild-type. This phenotype is in direct contrast to that of another regulatory protein, Klar; Klar's loss leads to the severe alteration of many properties of motion [12]. Thus, Klar, a proposed motor coordinator, and LSD2 must play mechanistically different roles. However, although the general machinery appears intact in the absence of LSD2, the machinery's ability to respond to regulatory signals is impaired.

LSD2 Can Physically Interact with a Component of the Transport Machinery

Klar is crucial for normal regulation of transport, and its droplet localization is mediated by its C-terminal LD domain [13]. Using Klar-LD as bait in a yeast two-hybrid assay, we screened a cDNA library from early embryos to identify proteins that can bind to Klar-LD. Among 33 positive clones out of 4 × 10^{6} milion screened (D.H.K.,

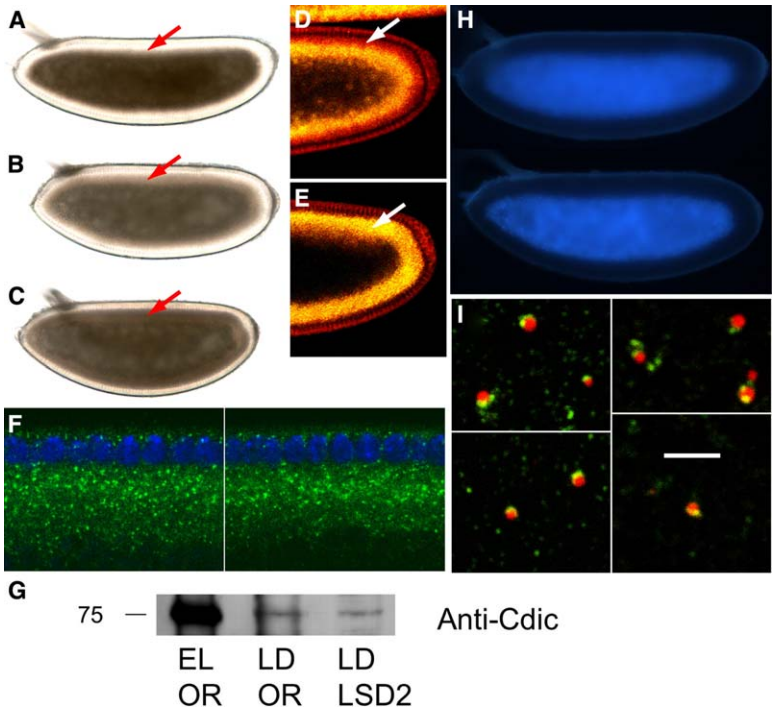

Figure 4. In *LSD2* Mutant Embryos, the Distribution of Lipid Droplets, but Not of Other Organelles, Is Altered

(A–C) Phase II embryos inspected by bright-field microscopy: Wild-type embryos (A), in which lipid droplets accumulate basally, have a much more transparent periphery than *halo*$^{-}$ embryos (C), in which lipid droplets accumulate apically. Transparency of *LSD2* mutants (*LSD2*^{KG}) was intermediate (B).

(D and E) Embryos were stained with the droplet-specific dye Nile red and examined by confocal microscopy. Yellow represents lipid droplets, and red is a diffuse cytoplasmic signal. Lipid droplets accumulate basally in the wild-type (D) and are found throughout the periphery in the *LSD2* mutant (E). The white arrow indicates the affected region.

(F) Distributions of nuclei (blue) and Golgi (green) are indistinguishable in wild-type (left) and *LSD2*^{KG} (right) embryos.

(G) Lysate from wild-type embryos (EL OR) and lipid droplets from both wild-type (LD OR) and *LSD2*^{KG} embryos (LD LSD2) were processed for Western blot analysis with anti-Cdic (90 μg of total proteins per lane).

(H) Distribution of yolk (blue) between wild-type (top) and *LSD2*^{KG} (bottom) embryos was indistinguishable.

(I) Lipid droplets from wild-type (left panels) and *LSD2*^{KG} (right panels) embryos were diluted away from other organelles and unattached motors by squashing embryos in buffer. Preparations were fixed and treated with the droplet-specific dye Nile red (red) and an antibody against Cdic, the intermediate chain of cytoplasmic dynein (green). In both cases, lipid droplets frequently had punctate Cdic signal next to them (see [10]). The scale bar represents 4 μm.

J.G.G., and M.A.W., unpublished data), we isolated a C-terminal fragment of LSD2. Both the library prey clone (LSD2 LC) and a full-length LSD2 prey interact with the Klar-LD construct, but not with a control bait lacking a cDNA insert (Figure 3J). Specific interactions between LSD2 and Klar result in the enhancement of transcription of both the *lacZ* and *LEU2* reporter genes in yeast (Figure 3J; data not shown). LSD2 has not been identified in screens of the same cDNA library for kinesin-1 interactors [28, 29], and no interactions with LSD2 have been identified in genome-wide interaction screens (Fly GRID database of 28,406 interactions;

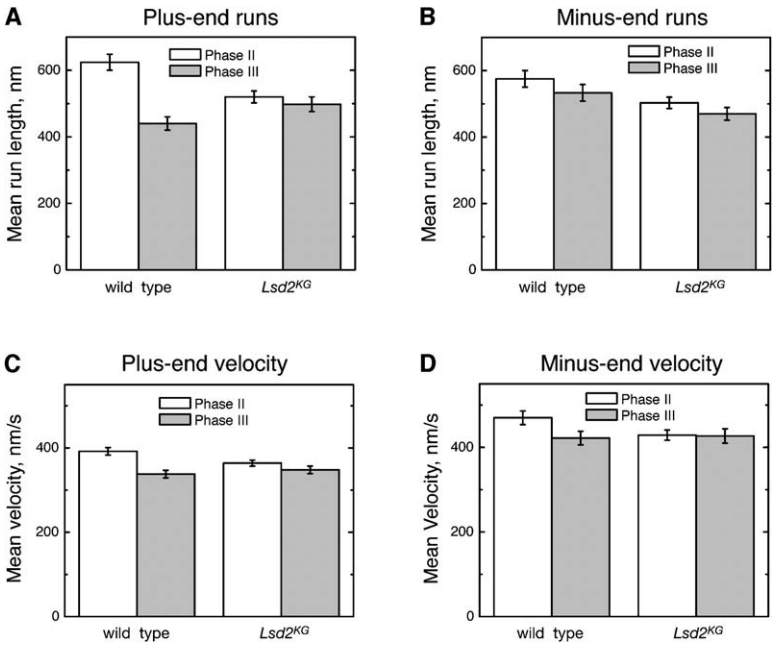

Figure 5. Comparison of Motion Parameters between Wild-Type and *LSD2*^{KG} Embryos

(A and B) Droplet motion in the mutant and wild-type displays run lengths of similar magnitude. The decrease in length of plus-end runs (A) observed in the wild-type between phases II and III (bars to left) fails to occur in *LSD2*^{KG} embryos (bars to right), in which there is no change whatsoever. For minus-end motion (B), loss of LSD2 function results in a slight overall decrease in run length.

(C and D) Mean velocities of lipid droplets in wild-type and *LSD2*^{KG} backgrounds are very similar; plus-end-directed (C) and minus-end-directed (D) motion is shown. This figure displays velocity of runs between 500 and 1000 nm in length in order to specifically analyze long-fast runs (see Loss of LSD2 Affects Specific Parameters of Droplet Motion). The values in Table 1, in contrast, are averages over all runs in a given direction. For the wild-type, there is slight decrease in velocity between phase II and phase III for both directions of travel. This decrease is absent in the *LSD2*^{KG} background. Error bars in (A)–(D) represent the SEM.

Table 1. Physical Parameters of Droplet Motion

	Mean Travel Distance (nm)	D_S (nm)	D_L (nm)	χ^2, P(χ^2)	Number Ratio R_{SL}	Velocity (nm/s)
Minus End						
Wild-type phase II (n = 1344)	575 ± 25	94 ± 7	981 ± 94	0.99, 0.50	2.0 ± 0.4	386 ± 6
LSD2^{KG} phase II (n = 1986)	503 ± 17	83 ± 7	714 ± 47	1.24, 0.10	1.5 ± 0.3	334 ± 4
Wild-type phase III (n = 1011)	533 ± 25	77 ± 6	1154 ± 146	1.1, 0.28	2.4 ± 0.5	320 ± 6
LSD2^{KG} phase III (n = 1351)	471 ± 19	82 ± 6	772 ± 61	1.0, 0.50	1.9 ± 0.4	333 ± 5
Plus End						
Wild-type phase II (n = 1293)	624 ± 24	68 ± 5	949 ± 62	0.78, 0.85	1.5 ± 0.3	325 ± 5
LSD2^{KG} phase II (n = 1801)	520 ± 18	74 ± 5	828 ± 52	0.96, 0.6	1.7 ± 0.3	301 ± 4
Wild-type phase III (n = 982)	441 ± 20	74 ± 7	604 ± 47	0.78, 0.85	1.4 ± 0.3	280 ± 4
LSD2^{KG} phase III (n = 1233)	498 ± 21	75 ± 7	833 ± 93	1.35, 0.05	2.3 ± 0.6	283 ± 4

Droplet location was determined as a function of time, and then custom software was employed to parse the motion into pauses and "runs," that is, periods of uninterrupted motion in a given direction. The distance constants D_S and D_L measure the average travel distance for short-slow and long-fast runs, respectively [10]. They result from fitting histograms of travel distance, D, to the sum of two decaying exponential functions: $y(D) = A_S e^{-D/D_S} + A_L e^{-D/D_L}$. The goodness of this fit is indicated by the χ^2 values and their corresponding probabilities. The number ratio R_{SL} measures the relative frequency of short-slow in relation to long-fast runs. Indicated errors for mean travel distance and velocity reflect the SEM, whereas the other uncertainties are derived from the fits.

http://biodata.mshri.on.ca/fly_grid); thus, LSD2 does not interact promiscuously with other proteins. This result suggests that LSD2 regulates the motors on lipid droplets by physically interacting with the coordinator Klar. Because both Klar and LSD2 are involved in the regulation of transport and reside on the surface of embryonic lipid droplets, we predict that these two molecules interact not only in the yeast system, but also in *Drosophila* embryos.

LSD2 Is Phosphorylated in a Halo-Dependent Manner

How might LSD2 enable regulation of motor activity? Although LSD2 had been identified owing to changes in its pattern on 2D gels, by Western analysis, total LSD2 levels per embryo displayed only minor changes between phases I, II, and III (Figure 6A, EL), even when compared to earlier stages ("phase 0"). LSD2 was also not differentially recruited to droplets from the surrounding cytoplasm in different phases because total LSD2 levels were very similar on droplets from all phases (Figure 6A, LD).

We therefore returned to 2D gel electrophoresis; we separated proteins in droplet preparations by molecular weight and isoelectric point (IEP) and subsequently probed for LSD2 by Western analysis (Figure 6B). In all phases, LSD2 was represented by a range of spots, of similar molecular weight, but ranging in IEP from 6.5 to 8.5. This suggests that LSD2 can exist in multiple isoforms distinguished by their IEP.

To test whether some or all of these isoforms were caused by phosphorylation, we treated the lipid-droplet fraction proteins with alkaline phosphatase to remove phosphate groups. All the spots of lower IEP were converted into a single spot at IEP 8.5 (Figure 6C). Thus, the right-most spot in untreated embryo lysates appears to be the unphosphorylated form of LSD2, and the other spots are caused by addition of various numbers of phosphates.

The pattern of LSD2 spots changed reproducibly with the phase of transport (Figure 6B, plus sign), raising the possibility that these modifications are responsible for the changes in droplet motion. We investigated a functional link between LSD2 phosphorylation and droplet motion in two ways. First, if the phosphorylation changes regulate droplet motion, they might be specific to moving droplets. We found that two independently isolated *Drosophila* cell lines, S2 and S3, contain abundant stationary lipid droplets (not shown). Purified lipid droplets from these cells had LSD2 that was predominantly unphosphorylated (Figure 6D). The pattern was very similar to that of the phosphatase-treated embryonic droplets (Figure 6C).

As a second test of functional relevance, we examined LSD2 phosphorylation in *halo*$^-$ embryos. Upregulation of Halo in phase II drives net plus-end transport [14]. Without Halo, phase II droplet motion is net minus-end directed (Figure 4C), like wild-type phase III. In relation to the wild-type, the LSD2 on droplets from phase II *halo*$^-$ embryos (Figure 6E) showed a pronounced increase in spots on the left end of the spectrum, representing lower IEP. It is these spots that in the wild-type change between phases II and III (Figure 6B). Thus, in the absence of Halo, the phosphorylation pattern of LSD2 in phase II approximates the pattern of the wild-type phase III; it mimics how droplet motion itself is altered in the absence of Halo. This observation strongly suggests that Halo controls droplet motion at least in part by altering LSD2's state of phosphorylation. The temporal correlation between upregulation of Halo and changes in LSD2 phosphorylation is consistent with rather direct effects of Halo on LSD2 (Figure 7).

Discussion

Using a biochemical approach, we identified a new regulator of droplet transport, LSD2, the *Drosophila* homolog of the mammalian Perilipin. In the absence of LSD2, droplets move bidirectionally, but the embryos lose the ability to initiate directed droplet transport. Our functional analysis suggests the first outline of a regulatory pathway for droplet motion, connecting LSD2, Halo,

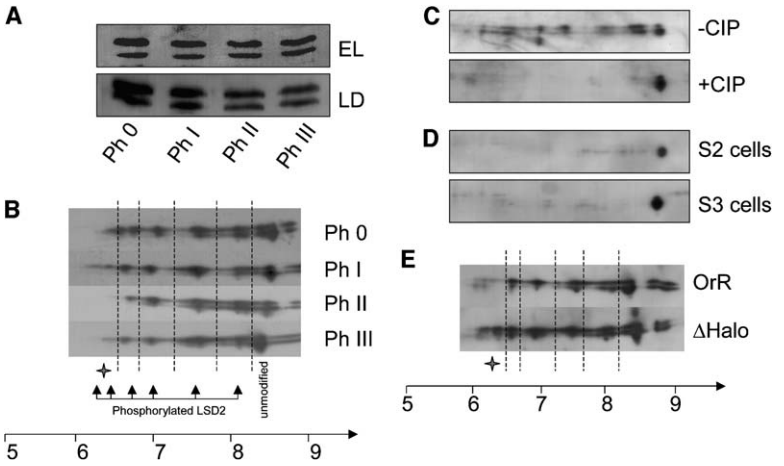

Figure 6. LSD2 Is Multiply Phosphorylated in a Phase- and Halo-Dependent Manner

(A) LSD2 levels on lipid droplets purified from different phases of development. Equal amounts of proteins (50 μg/lane) of whole embryo lysates (EL, top) and lipid droplets (LD, bottom), specific for each phase of development, were separated by gel electrophoresis and then subjected to immunoblot analysis with anti-LSD2. There was no significant change in overall level of LSD2 between phases.

(B) Lipid droplets from phases 0, I, II, and III were isolated, and 65 μg of protein each was analyzed by 2D electrophoresis and Western blotting with anti-LSD2 antibody. The 42–44 kDa region of each gel is shown; LSD2 is present as a series of spots of varying pIs. The plus sign indicates the location where reproducible changes in spot intensity were observed between phases. All these spots represent LSD2 because they are essentially gone on similar Western blots with droplet preparations from *LSD2*^{KG} embryos (not shown).

(C) After phosphatase treatment (+CIP), only one isoform of LSD2 was detected by 2D gel analysis. The disappearance of the other isoforms of LSD2, characteristic of the untreated sample (–CIP), confirmed that LSD2 is phosphorylated. In contrast to (B), the lipid droplets were isolated from embryos representing phases 0–III in order to confirm that all the additional spots in each phase were due to phosphorylation.

(D) The LSD2 on lipid droplets purified from *Drosophila* S2 and S3 cells (in which droplets do not move) is not phosphorylated. Lipid droplets from S2 cells (top) have less LSD2 than lipid droplets from S3 cells (bottom), so different amounts of total protein were used for good detection of LSD2 (top, 110 μg; bottom, 35 μg).

(E) LSD2 expression on lipid droplets (65 μg) from phase II wild-type (OR) and phase II *halo*$^{-}$ embryos (*Δhalo*). The spot patterns in *halo*$^{-}$ embryos resemble LSD2 signal from the phase III wild-type. The plus sign indicates changes in spot intensity.

Klar, and phosphorylation. These observations have implications both for the function of LSD2 and for the control of lipid distribution and metabolism. The role of LSD2 as a cargo-specific transport regulator may provide a paradigm for how different cargoes can employ the same set of opposite-polarity motors to move through the same cytoplasm yet be controlled independently.

Regulation of Transport

LSD2 is critical for the ability to control the direction of net transport of lipid droplets because in its absence such control is lost. The physical parameters of droplet motion in *LSD2* mutant embryos are consistent with the lack of net transport: Mean travel distances in either direction are very similar to each other in both phases II and III.

Two observations suggest how LSD2 could mediate this regulation. First, LSD2 is present on the droplets and can physically interact with Klar, so it could directly interact with the motor machinery. Second, LSD2 is posttranslationally modified depending on the phase of transport (Figure 6). These modifications appear to be functionally important because they change with the phase of transport, are absent in unmoving droplets, and are altered in a consistent way when Halo is absent. Thus, LSD2 is likely a target of the developmentally controlled regulatory pathways that act on the droplet transport machinery. LSD2 is found all over the surface of embryonic lipid droplets (Figure 3), whereas components of the core motor machinery (Klar, dynein) are present in single punctae per droplet ([10, 13]; see also Figure 4). Because only a small fraction of total LSD2 changes its phosphorylation state from phase to phase (Figure 6), it is likely that only the LSD2 molecules in the direct vicinity of the motors mediate this regulatory signal.

LSD2 might be an integral part of the motor complexes, in which it would physically touch the motor machinery and help to position the motors in the correct 3D arrangement to each other (Figures 7A and 7B). Different modified forms of LSD2 could increase or decrease the probability of a motor to end a run by sterically favoring or disfavoring how the motor reaches the track (Figures 7B and 7C). Thus, without LSD2, the switching mechanism that engages or disengages motors [10] is intact, but its properties cannot be modified. Alternatively, LSD2 could be required to position an external factor such as a kinase to control motor activity. The different forms of LSD2 could then either change their affinity for the factor or position the kinase next to different targets.

Because LSD2 is predominantly or exclusively localized to lipid droplets [21, 24, 27], and regulation fails in its absence, it appears to represent a key component that allows lipid-droplet transport to be regulated in a cargo-specific manner, independently of the transport of other cargoes. If LSD2 relays regulatory input to the motors, then only the motors on lipid droplets will respond to these signals. LSD2 is therefore an "add-on" protein because the proteins responsible for motor coordination and switching appear to function relatively normally in its absence, although they have lost the ability to respond to their normal inputs. This interpretation suggests functional differentiation in the transport machinery: a core complex of opposite-polarity motors, possibly shared between different cargoes, that receives its "marching orders" through a cargo-specific regulator not directly involved in motor function. If this hypothesis is correct, then other cargoes should carry

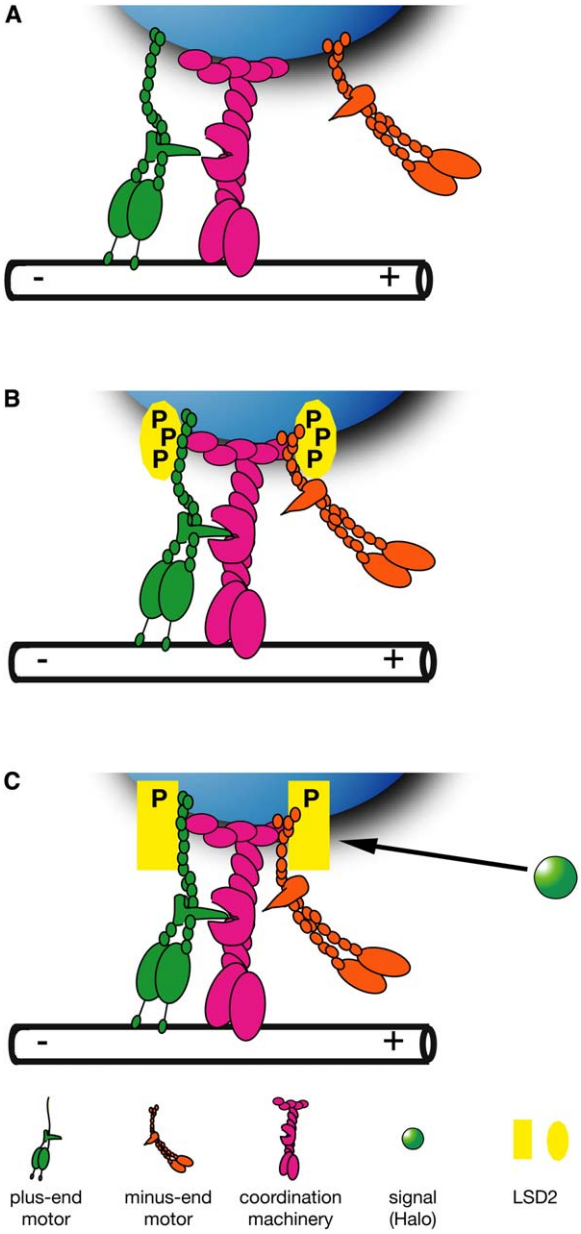

Figure 7. Models for LSD2 Function

(A) In the absence of LSD2, motors are not held in the correct orientation to each other.

(B) LSD2 may cluster the motors and the rest of the motor machinery into functional complexes.

(C) In response to signals, LSD2's phosphorylation state changes, resulting in an altered conformation. This alteration is transmitted to the motors or coordination machinery.

analogous "conductor" molecules that act to transmit regulatory input just as LSD2 does on lipid droplets.

Conceptually, such conductor molecules are at a crucial position in the pathways that regulate motion: They are expected to be the targets of cargo-specific signaling events and connect up with the core motor machinery shared between many cargoes. For lipid droplets, our results suggest a pathway where the transacting signal Halo controls the phosphorylation state of LSD2, which in turn contacts Klar, a proposed component of the motor machinery. This model makes testable predictions about how components of the regulatory machinery interact physically and functionally during droplet transport. It may also serve as a paradigm for other cargo transport; for example, it suggests how kinase cascades affect the activities of opposite-polarity motors. For lipid-droplet transport, several independent lines of evidence suggest that phosphorylation of LSD2 is a key regulatory step; understanding the details of how LSD2 phosphorylation is related to changes in transport will therefore likely be a next crucial step for dissecting the mechanisms of regulation.

Molecular Mechanism of LSD2 Action

LSD2 is a member of the PAT protein family, which is present in species from slime molds to mammals [24]. All tested family members localize to the surface of lipid droplets. Both insects and mammals express multiple family members, suggesting that PAT proteins are functionally specialized. The best-studied PAT protein is the mammalian Perilipin, which keeps lipid breakdown to a low level by preventing access of lipases to the droplets' neutral lipids. After hormonal signaling, Perilipin is multiply phosphorylated, which allows lipases to dock to the droplet surface and subsequently break down the neutral lipids; mice lacking Perilipin display severe defects in lipid metabolism [25, 30]. It is thought that phosphorylation induces LSD2 conformational changes that directly or indirectly give lipases access to the droplet core [31].

Because LSD2 in *Drosophila* functions in controlling lipid homeostasis [21, 22] similarly to Perilipin and because we found evidence for multiple, developmentally regulated phosphorylation events, LSD2 may undergo similar conformational changes. It is therefore possible that a shared molecular mechanism, phosphorylation of LSD2, controls both lipid metabolism and droplet motion.

A Link between Transport and Lipid Homeostasis?

There has been no systematic documentation of the extent of lipid-droplet transport, but droplets display active motion in disparate cells, including embryos of *Drosophila* and of the fish Medaka [19], in mammary glands, and in a range of mammalian cell lines [18]. In each case, microtubule-based transport has been implicated as responsible for the motion [19, 20, 32–34]. In fibroblasts, for example, lipid droplets move bidirectionally along microtubules, and the dynein cofactor dynactin is crucial for both minus- and plus-end motion [20], suggesting tightly coordinated motors just as in *Drosophila* embryos. Because the PAT family of proteins is broadly conserved, we hypothesize that like LSD2, members of this family regulate these various instances of lipid-droplet motion.

Is it a coincidence that lipid metabolism and microtubule-based motion are controlled via the same key molecule? Available evidence suggests functional links. First, when lipolysis is stimulated in adipocytes, droplets fragment and disperse throughout the cell [16, 35]. Fragmentation results in a vast increase in droplet sur-

face area, making attack by lipases much more efficient. Second, dispersion could put droplets in contact with other organelles, such as mitochondria, important for the catabolic breakdown of lipids. Indeed, mitochondria often surround lipid droplets in clusters [36]. The mechanisms leading to fragmentation and dispersion are unknown, but active pulling by motors to deform and move droplets is an intriguing possibility. When lipolysis is stimulated, many proteins are newly recruited to the droplets, among them Rab proteins [35], a class of proteins with roles in regulating cargo transport [37, 38].

This emerging link between the physical motion of droplets and lipid metabolism opens exciting new possibilities: Perhaps impaired droplet transport contributes to metabolic diseases. Once we understand the mechanisms underlying droplet motion, it will be possible to specifically disrupt droplet motion and directly test its contribution to lipid metabolism.

Conclusion

We find that the lipid-droplet-associated protein LSD2 is required to regulate the motor-driven motion of lipid droplets in *Drosophila* embryos. In its absence, droplets move in a robust way, but their motion cannot be regulated. These observations suggest that it is possible to separate the mechanisms that govern bidirectional transport into two functionally distinct but related parts: a motor-control cassette that turns motors on and off and a regulatory cassette that is cargo specific and controls when and how the motor-control cassette alters its activity. For lipid droplets, we propose that LSD2 is an essential component of this regulatory cassette and that the functional state of the regulatory cassette is in part controlled by Halo-dependent changes in LSD2 phosphorylation. LSD2, like its mammalian homolog Perilipin, can also control lipid homeostasis, suggesting the intriguing possibility that droplet motion plays a role in the control of lipid metabolism.

Experimental Procedures

Embryo Collection

Embryos were collected for 1 hr and aged for various times (1.5 hr, 2.5 hr, and 3.5 hr) to obtain samples highly enriched in phase I, phase II, or phase III embryos, respectively. An initial embryo collection was discarded to eliminate fertilized eggs that females might have been storing.

Isolation of Lipid Droplets by Subcellular Fractionation

Lipid droplets were purified as described [23] with few modifications. In brief, embryo or cell lysates were loaded on a sucrose gradient solution. After ultracentrifugation, the buoyant lipid droplets were collected from the top of the gradient. Isolated lipid droplets were either solubilized in SDS-containing buffer for subsequent SDS-PAGE or resuspended in RIPA buffer (25 mM HEPES, 1% deoxycholate, 1% NP-40, 0.2% SDS, 1 mM sodium orthovanadate, glycerol, and 30 mM sodium pyrophosphate) for 2D gel electrophoresis. For details on the 2D electrophoresis, phosphatase treatment, and immunoblot analysis, see the Supplemental Experimental Procedures.

Anti-LSD2 Antibody

Rabbits were repeatedly immunized with the peptide GTNVEQSG GSSSDACSP (aa 296–312 in the LSD2 protein sequence) by a commercial facility (Washington Biotechnology). Crude serum was used for immunoblotting. For immunocytochemistry, serum was first incubated with fixed *LSD2^{KG}* embryos to remove crossreacting antibodies. Immunostaining was performed with a variation of standard procedures (see Supplemental Experimental Procedures).

Particle Tracking and Analysis

Droplet motion was recorded and analyzed essentially as described [10]. See the Supplemental Experimental Procedures for details.

Supplemental Data

Detailed Experimental Procedures, as well as two supplemental figures, are available at http://www.current-biology.com/cgi/content/full/15/14/1266/DC1/.

Acknowledgments

We thank the Bloomington Stock Center for fly stocks. We thank O. Kamal for help with fly genetics and sequencing, A. L. Wong for her work tracking lipid droplets, and M. Zapata for helping with the yeast two-hybrid screen. This work was supported by National Institute of General Medical Sciences (NIGMS) grant GM 64624-01 to S.P.G., a Kimmel Scholar Award (Sidney Kimmel Foundation for Cancer Research) and NIGMS grant GM64687 to M.A.W., and National Science Foundation award 0342761 to J.G.G. Confocal microscopy was made possible by National Institutes of Health Shared Instrumentation Grant S10RR16780.

Received: June 13, 2005
Accepted: June 14, 2005
Published: July 26, 2005

References

1. Gross, S.P. (2004). Hither and yon: A review of bi-directional microtubule-based transport. Physical Biology *1*, 1–11.
2. Welte, M.A. (2004). Bidirectional transport along microtubules. Curr. Biol. *14*, R525–R537.
3. Chada, S.R., and Hollenbeck, P.J. (2004). Nerve growth factor signaling regulates motility and docking of axonal mitochondria. Curr. Biol. *14*, 1272–1276.
4. Smith, G.A., Gross, S.P., and Enquist, L.W. (2001). Herpes viruses use bidirectional fast-axonal transport to spread in sensory neurons. Proc. Natl. Acad. Sci. USA *98*, 3466–3470.
5. Smith, G.A., Pomeranz, L., Gross, S.P., and Enquist, L.W. (2004). Local modulation of plus-end transport targets herpesvirus entry and egress in sensory axons. Proc. Natl. Acad. Sci. USA *101*, 16034–16039.
6. Nascimento, A.A., Roland, J.T., and Gelfand, V.I. (2003). Pigment cells: A model for the study of organelle transport. Annu. Rev. Cell Dev. Biol. *19*, 469–491.
7. Rodionov, V., Yi, J., Kashina, A., Oladipo, A., and Gross, S.P. (2003). Switching between microtubule- and actin-based transport systems in melanophores is controlled by cAMP levels. Curr. Biol. *13*, 1837–1847.
8. Gross, S.P., Tuma, M.C., Deacon, S.W., Serpinskaya, A.S., Reilein, A.R., and Gelfand, V.I. (2002). Interactions and regulation of molecular motors in Xenopus melanophores. J. Cell Biol. *156*, 855–865.
9. De Vos, K.J., Sable, J., Miller, K.E., and Sheetz, M.P. (2003). Expression of phosphatidylinositol (4,5) bisphosphate-specific pleckstrin homology domains alters direction but not the level of axonal transport of mitochondria. Mol. Biol. Cell *14*, 3636–3649.
10. Gross, S.P., Welte, M.A., Block, S.M., and Wieschaus, E.F. (2000). Dynein-mediated cargo transport in vivo. A switch controls travel distance. J. Cell Biol. *148*, 945–956.
11. Gross, S.P., Welte, M.A., Block, S.M., and Wieschaus, E.F. (2002). Coordination of opposite-polarity microtubule motors. J. Cell Biol. *156*, 715–724.
12. Welte, M.A., Gross, S.P., Postner, M., Block, S.M., and Wieschaus, E.F. (1998). Developmental regulation of vesicle transport in *Drosophila* embryos: Forces and kinetics. Cell *92*, 547–557.

13. Guo, Y., Jangi, S., and Welte, M.A. (2005). Organelle-specific control of intracellular transport: Distinctly targeted isoforms of the regulator Klar. Mol. Biol. Cell *16*, 1406–1416.
14. Gross, S.P., Guo, Y., Martinez, J.E., and Welte, M.A. (2003). A determinant for directionality of organelle transport in *Drosophila* embryos. Curr. Biol. *13*, 1660–1668.
15. Brown, D.A. (2001). Lipid droplets: Proteins floating on a pool of fat. Curr. Biol. *11*, R446–R449.
16. Londos, C., Brasaemle, D.L., Schultz, C.J., Segrest, J.P., and Kimmel, A.R. (1999). Perilipins, ADRP, and other proteins that associate with intracellular neutral lipid droplets in animal cells. Semin. Cell Dev. Biol. *10*, 51–58.
17. Zweytick, D., Athenstaedt, K., and Daum, G. (2000). Intracellular lipid particles of eukaryotic cells. Biochim. Biophys. Acta *1469*, 101–120.
18. Targett-Adams, P., Chambers, D., Gledhill, S., Hope, R.G., Coy, J.F., Girod, A., and McLauchlan, J. (2003). Live cell analysis and targeting of the lipid droplet-binding adipocyte differentiation-related protein. J. Biol. Chem. *278*, 15998–16007.
19. Webb, T.A., Kowalski, W.J., and Fluck, R.A. (1995). Microtubule-based movements during ooplasmic segregation in the Medaka fish egg (Oryzias latipes). Biol. Bull. *188*, 146–156.
20. Valetti, C., Wetzel, D.M., Schrader, M., Hasbani, M.J., Gill, S.R., Kreis, T.E., and Schroer, T.A. (1999). Role of dynactin in endocytic traffic: Effects of dynamitin overexpression and colocalization with CLIP-170. Mol. Biol. Cell *10*, 4107–4120.
21. Teixeira, L., Rabouille, C., Rorth, P., Ephrussi, A., and Vanzo, N.F. (2003). Drosophila Perilipin/ADRP homologue Lsd2 regulates lipid metabolism. Mech. Dev. *120*, 1071–1081.
22. Grönke, S., Beller, M., Fellert, S., Ramakrishnan, H., Jackle, H., and Kuhnlein, R.P. (2003). Control of fat storage by a *Drosophila* PAT domain protein. Curr. Biol. *13*, 603–606.
23. Yu, W., Cassara, J., and Weller, P.F. (2000). Phosphatidylinositide 3-kinase localizes to cytoplasmic lipid bodies in human polymorphonuclear leukocytes and other myeloid-derived cells. Blood *95*, 1078–1085.
24. Miura, S., Gan, J.W., Brzostowski, J., Parisi, M.J., Schultz, C.J., Londos, C., Oliver, B., and Kimmel, A.R. (2002). Functional conservation for lipid storage droplet association among perilipin-, ADRP-, and TIP 47-related proteins in mammals, Drosophila, and Dictylostelium. J. Biol. Chem. *277*, 32253–32257. Published online June 20, 2002.. 10.1074/jbc.M204410200
25. Tansey, J.T., Sztalryd, C., Gruia-Gray, J., Roush, D.L., Zee, J.V., Gavrilova, O., Reitman, M.L., Deng, C.X., Li, C., Kimmel, A.R., et al. (2001). Perilipin ablation results in a lean mouse with aberrant adipocyte lipolysis, enhanced leptin production, and resistance to diet-induced obesity. Proc. Natl. Acad. Sci. USA *98*, 6494–6499.
26. Lu, X., Gruia-Gray, J., Copeland, N.G., Gilbert, D.J., Jenkins, N.A., Londos, C., and Kimmel, A.R. (2001). The murine perilipin gene: The lipid droplet-associated perilipins derive from tissue-specific, mRNA splice variants and define a gene family of ancient origin. Mamm. Genome *12*, 741–749.
27. Fauny, J.D., Silber, J., and Zider, A. (2005). Drosophila Lipid Storage Droplet 2 gene (Lsd-2) is expressed and controls lipid storage in wing imaginal discs. Dev. Dyn. *232*, 725–732.
28. Gindhart, J.G., Chen, J., Faulkner, M., Gandhi, R., Doerner, K., Wisniewski, T., and Nandlestadt, A. (2003). The kinesin-associated protein UNC-76 is required for axonal transport in the Drosophila nervous system. Mol. Biol. Cell *14*, 3356–3365.
29. Wisniewski, T.P., Tanzi, C.L., and Gindhart, J.G. (2003). The Drosophila kinesin-I associated protein YETI binds both kinesin subunits. Biol. Cell. *95*, 595–602.
30. Martinez-Botas, J., Anderson, J.B., Tessier, D., Lapillonne, A., Chang, B.H., Quast, M.J., Gorenstein, D., Chen, K.H., and Chan, L. (2000). Absence of perilipin results in leanness and reverses obesity in Lepr(db/db) mice. Nat. Genet. *26*, 474–479.
31. Zhang, H.H., Souza, S.C., Muliro, K.V., Kraemer, F.B., Obin, M.S., and Greenberg, A.S. (2003). Lipase-selective functional domains of perilipin A differentially regulate constitutive and protein kinase A-stimulated lipolysis. J. Biol. Chem. *278*, 51535–51542.
32. Morales, C.R., Domitrovic, H.A., and Sampietro, J. (1982). Influence of colchicine on lactating mammary gland of the cow and rat with special reference to the exocytosis and to the milk fat globule secretion. Anat. Histol. Embryol. *11*, 56–64.
33. Nickerson, S.C., Smith, J.J., and Keenan, T.W. (1980). Role of microtubules in milk secretion—Action of colchicine on microtubules and exocytosis of secretory vesicles in rat mammary epithelial cells. Cell Tissue Res. *207*, 361–376.
34. Wu, C.C., Howell, K.E., Neville, M.C., Yates, J.R., 3rd, and McManaman, J.L. (2000). Proteomics reveal a link between the endoplasmic reticulum and lipid secretory mechanisms in mammary epithelial cells. Electrophoresis *21*, 3470–3482.
35. Brasaemle, D.L., Dolios, G., Shapiro, L., and Wang, R. (2004). Proteomic analysis of proteins associated with lipid droplets of basal and lipolytically stimulated 3T3–L1 adipocytes. J. Biol. Chem. *279*, 46835–46842.
36. Novikoff, A.B., Novikoff, P.M., Rosen, O.M., and Rubin, C.S. (1980). Organelle relationships in cultured 3T3–L1 preadipocytes. J. Cell Biol. *87*, 180–196.
37. Barbero, P., Bittova, L., and Pfeffer, S.R. (2002). Visualization of Rab9-mediated vesicle transport from endosomes to the trans-Golgi in living cells. J. Cell Biol. *156*, 511–518.
38. van Ijzendoorn, S.C., Mostov, K.E., and Hoekstra, D. (2003). Role of rab proteins in epithelial membrane traffic. Int. Rev. Cytol. *232*, 59–88.